Asociación Argentina
de Mecánica Computacional

Mecánica Computacional Vol XXIX, págs. 5691-5704 (artículo completo)
Eduardo Dvorkin, Marcela Goldschmit, Mario Storti (Eds.)
Buenos Aires, Argentina, 15-18 Noviembre 2010

A NUMERICAL INVESTIGATION OF STABILIZED METHANE/Air COMBUSTION AND POLLUTANTS FORMATION IN POROUS BURNERS

Roberto Carlos Moro Filho [a], **Amilcar Porto Pimenta** [b]

[a] *Escola de Ciencias e Tecnologia , Universidade Federal do Rio Grande do Norte, Caixa Postal 1524, Campus Universitário Lagoa Nova, CEP 59072-970, Natal/RN - Brasil, moro@ect.ufrn.br.*

[b] *Divisão de Engenharia Aeronáutica-IEA,* Instituto Tecnológico de Aeronáutica, *CEP 12228-900, São José dos Campos/SP- Brasil, amilcar@ita.br*

Keywords: porous media burner, premixed flame, numerical simulation.

Abstract. The technique of combustion in porous media offers advantages comparing with free flame burners. High burning rates, flame stability, and low pollutant emissions are some of the main characteristics of porous burners. The present work presents numerical simulations of combustion in porous media. A laminar two dimensional model is based on a macroscopic formulation of the transport equations. A 6 step reduced mechanism was utilized to model the chemical kinetics. Finite volume method is used for simulation with a boundary-fitted non-orthogonal coordinate system. A radiant porous burner is simulated and a sensitivity study to the Rosseland mean attenuation coefficient, to the thermal conductivity of the solid and to the porosity is presented. It is shown that the properties of the pre-heating region not affect, significantly, the CO emissions at the exit of the reactor, while the properties of the combustion region has a strong influence.

1. INTRODUCTION

There has been an interest in combustion within porous media due to the needs of industry focusing efficiency and reduction of emission of pollutants. Premixed combustion inside a porous medium is currently under investigation due to the characteristics of this technology which provides controlled flames. Systems based on fluidized bed combustion, in-situ combustion for oil recovery, household heating combustion, are just a few examples of such applications (Trimis and Durst, 1996).

Weinberg (1971) introduced the idea of utilize part of the energy of the combustion products to preheat the incoming reactants. The recuperation causes a net transfer of enthalpy from the burned gases to the unburned gases and consequently makes possible to achieve a local peak temperature higher than the adiabatic flame temperature. The recirculation or recuperation of heat causes the extension of the lean flammability limit and the high reaction rates. In the literature the flames that have peaks of temperature higher than the adiabatic flame temperature are named 'excess enthalpy flames' (Howell et al., 1996).

In most of the studies of premixed combustion within inert porous media the flow is assumed to be laminar and one-dimensional, the variation in the pressure across the flame is generally negligible compared with the absolute pressure, and the pressure is assumed constant (Baek, 1989; Yoshizawa et al., 1988; Hsu et al., 1993; Neef et al., 1999). The use of single-step global chemistry (Mohamad et al., 1994; Sathe et al., 1990; Baek, 1989) is common, but, the inadequacies of global kinetics are well recognized. Hsu et al. (1993) presents a comparison between one-step and multi-step chemistry.

Studies on macroscopic transport modeling of incompressible flows in porous media have been based on the volume-average methodology for either heat or mass transfer (Kaviany, 1995; Bear, 1972). Because of important influence of lateral heat loss in porous medium burners, a two dimensional model is necessary (Brenner et al., 2000).

The present paper follows the foregoing works and presents a two dimensional mathematical model for laminar premixed flame combustion in porous media. The numerical methodology employed is based on the control-volume approach with a boundary-fitted non-orthogonal coordinate system. In order to achieve steady combustion in the porous media the reactors have a steep gradient in the pore size of the porous matrix. The reactor studied in this work have two regions, with a small pore size in the first region and a large pore size downstream in the second region. The flame can be stabilized at the interface between the two different porosity blocks. The main goal of this study is to investigate the choice of materials in each porous region, pre-heating region and combustion region, and the influence of this choice on the pollutants emission. Thermal nonequilibrium was subject of previous work (Moro Filho and Pimenta, 2009). Dispersion is subject of ongoing investigations and will be addressed in subsequent paper.

A sensitivity study to the Rosseland mean attenuation coefficient, to the thermal conductivity of the solid and to the porosity is presented. The purpose is to discover the influence of the choice of the materials employed in which region, pre-heating region and combustion region, on the pollutants emission.

2. MACROSCOPIC TRANSPORT EQUATIONS

2.1. Macroscopic continuity equation

$$\phi \frac{\partial \rho}{\partial t} + \nabla.(\rho \mathbf{u}_{\mathrm{D}}) = 0 \tag{1}$$

where, $\mathbf{u}_{\mathrm{D}}$ is the average surface velocity (also known as seepage, superficial, filter or Darcy velocity). Equation (1) represents the macroscopic continuity equation for an incompressible fluid.

2.2. Macroscopic momentum equation

The heuristic macroscopic momentum equation utilized in this work is found in the literature (Kaviany, 1995; Pedras, 2000) and corresponds to an attempt of the scientific community to develop an equation, based on a volume-averaged treatment of the flow field, along the lines of Navier-Stokes equation. Another desirable characteristic of this heuristic equation is that it can describe both the momentum transport through the porous media as well as that in the plain media.

$$\frac{\partial(\rho \mathbf{u}_{\mathrm{D}})}{\partial t} + \nabla \cdot \left(\frac{\rho \mathbf{u}_{\mathrm{D}} \mathbf{u}_{\mathrm{D}}}{\phi} \right) = -\nabla(\phi p) + \mu \nabla^2 \mathbf{u}_{\mathrm{D}} - \left[\frac{\mu \phi}{K} \mathbf{u}_{\mathrm{D}} + \frac{c_F \phi \rho |\mathbf{u}_{\mathrm{D}}| \mathbf{u}_{\mathrm{D}}}{\sqrt{K}} \right] \tag{2}$$

where the last two terms in equation (2), represent the Darcy-Forchheimer contribution (Pedras, 2000). The symbol K is the porous medium permeability, $c_F = 0.55$ is the form drag coefficient (Forchheimer coefficient), p is the intrinsic (volume-averaged on fluid phase) pressure of the fluid, ρ is the fluid density and is a function of temperature, μ represents the fluid dynamic viscosity and ϕ is the porosity of the porous medium.

2.3. Macroscopic Energy Equation

$$\begin{aligned} &\left\{ \left(\rho c_p\right)_f \phi + \left(\rho c_p\right)_s (1-\phi) \right\} \frac{\partial T}{\partial t} + \left(\rho c_p\right)_f \nabla \cdot \left(\mathbf{u}_D T\right) = \\ &\nabla \cdot \left\{ \mathbf{K}_{eff,f} \cdot \nabla T \right\} + \phi \sum_{k=1}^{Nsp} \dot{w}_k M_k h_k \end{aligned} \tag{3}$$

where, T is the averaged temperature for both the solid and the liquid according to the concept of local thermal equilibrium (Kaviany, 1995; Rocamora, 2001), h_k is the specific enthalpy of species k, w_k is the molar rate of reaction of species k, M_k is the molecular weight of species k, K_{eff} is the effective conductivity tensor given by,

$$\mathbf{K}_{eff} = \left\{ \phi k_f + (1-\phi) \left[k_s + \frac{16\sigma(T)^3}{3K_r} \right] \right\} \mathbf{I} + \underbrace{\mathbf{K}_{tor}}_{tortuosity} + \underbrace{\mathbf{K}_{disp}}_{dispersion} \tag{4}$$

where, k_f and k_s are the thermal conductivities for the fluid and for the solid, K_r is the local Rosseland mean attenuation coefficient, σ is the Stefan-Boltzmann constant, $\mathbf{K}_{tor}$ and $\mathbf{K}_{disp}$

are the tortuosity and thermal dispersion conductivity tensors, respectively.

The radiation in an optically dense medium can be modeled using the diffusion approximation or Rosseland model (Siegel and Howell, 2002). In the radiative diffusion approximation the radiation is computed like an increase in the effective conductivity and is represented by the term containing K_r in equation (4). For a combustion occurring inside a ceramic, with a small solid conductivity like Zirconium Oxide, the conductivity due to radiation can represent more than 80% of the total conductivity, hence, radiation within the porous media cannot be neglected.

In this work the effects of dispersion and tortuosity are neglected, hence, the last two terms on the right in equation 4 are not being considered.

2.4. Macroscopic Mass Transport Equation

$$\frac{\partial(\rho\phi y_k)}{\partial t} + \nabla\cdot(\rho\mathbf{u}_D y_k) = \nabla\cdot[\rho\mathbf{D}_{eff}\cdot\nabla(\phi y_k)] + \phi\dot{w}_k M_k \tag{5}$$

where y_k is the local mass fraction for the species k. The effective dispersion tensor D_{eff} is defined as:

$$\mathbf{D}_{eff} = \mathbf{D}_{disp} + \mathbf{D}_{diff} = \mathbf{D}_{disp} + \frac{1}{\rho}\left(\frac{\mu}{Sc}\right)\mathbf{I} \tag{6}$$

where, Sc is the Schimidt number, D_{diff} is the macroscopic diffusion tensor, and D_{disp} is the mass dispersion tensor (Mesquita, 2003). The effects of dispersion are neglected in this work, therefore, the effective dispersion tensor is given by:

$$\mathbf{D}_{eff} = \frac{1}{\rho}\left(\frac{\mu}{Sc}\right)\mathbf{I} \tag{7}$$

2.5. Boundary conditions

The figure 1 presents the boundary conditions to the cylindrical porous burner, where: $\dot{q}_s$ is the heat flux at the exit, $\dot{q}_r$ the heat flux due to the radiation and $\dot{q}_w$ the heat flux at the wall of the burner. The surface of the packed bed radiates energy to the surrounding surfaces according to the equation bellow:

$$\dot{q}_r = -K_{eff}\frac{\partial T}{\partial x} = \left(\varepsilon_{eff}\sigma T^4 - \alpha_{eff}\sigma T_\infty^4\right) \tag{8}$$

where, ε_{eff} is effective emissivity, α_{eff} is the effective absorptivity of the porous bed and T_∞ is the ambient temperature. The ε_{eff} and α_{eff} are equal to simplify the solution.

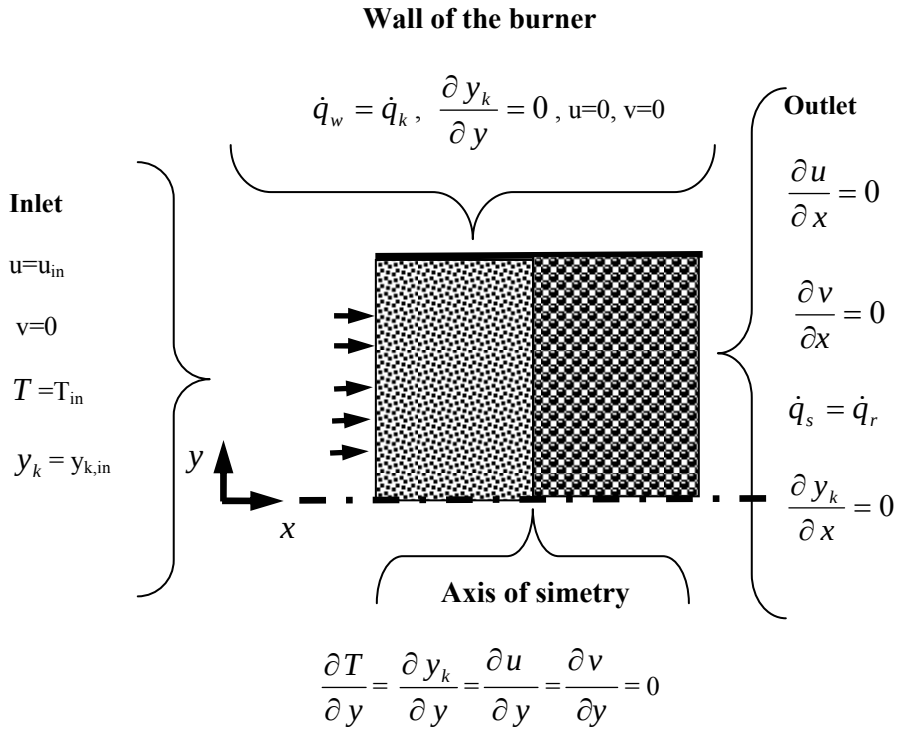

Figure 1. Boundary conditions.

2.6. Combustion model

The method to solve the chemical kinetic problem utilizes two models to describe the reaction process, a global reaction mechanism is used as a first approximation, following a six step reaction mechanism.

2.6.1. One-step global mechanism

The combustion reaction is assumed to occur in a single step according to the chemical equation

$$CH_4 + 2(1+\Psi)(O_2 + 3.76N_2) \longrightarrow CO_2 + 2H_2O + 2\Psi O_2 + 7.52(1+\Psi)N_2 \tag{9}$$

where, ψ is the excess air in the reactant stream at the inlet of porous foam and is related to the equivalence ratio Φ by,

$$\Psi = \frac{1}{\Phi} - 1 \tag{10}$$

where,

$$\Phi = \frac{(y_{fu} / y_{ox})}{(y_{fu} / y_{ox})_{st}} \tag{11}$$

The ratio of fuel consumption is given by,

$$S_{fu} = \rho^2 A y_{fu} y_{Ox} \exp(-E_a / RT) \tag{12}$$

where, A is the pre-exponential factor, Ea is the activation energy and R is the universal gas

constant. The gas density is updated using the ideal gas equation in the form,

$$\rho = P_0 / R^* T \tag{13}$$

where, P_0 is a reference pressure, which is kept constant during the relaxation process, and $R^* = R / M$ and M is the gas molecular mass.

2.6.2. Six-step reduced mechanism

Chang and Chen have developed a six-step reduced mechanism with an automatic computer code (CARM) from GRI-MECH 1.2:

(I) 2O = O2
(II) H + O = OH
(III) H2 + O = H + OH
(IV) O + (1/2) CH4 = (1/2) H2 + (1/2) H + (1/2) OH + (1/2) CO
(V) O + CO = CO2
(VI) O + H2O + (1/4) CO = (1/4) H2 + (1/4) H + O2 + (1/4) OH + (1/4) CH4

3. NUMERICAL MODEL

The governing equations were discretized using the finite volume procedure (Patankar, 1980) with a boundary-fitted non-orthogonal coordinate system. The system of algebraic equations was solved through the semi-implicit procedure according to Stone (1968). The SIMPLE algorithm for the pressure-velocity coupling was adopted to correct both the pressure and the velocity fields. The process starts with the solution of the two momentum equations. Then the velocity field is adjusted in order to satisfy the continuity principle. This adjustment is obtained by solving the pressure correction equation. The energy and species equations are solved using a fractional time step method (Yanenko, 1971) to eliminate the problems arising from the stiffness of the system. It was adopted the minimum residence time of the gas in all control volumes as the integration time step. Calculations start using one-step global kinetics mechanism, when the residuals reach $1x10^{-3}$ the multistep mechanism is switched on and the fractional time step method is applied (Malico *et al.*, 2000). The kinetic problem is solved using the Chemkin 4.1 (Kee et al., 2004) with a six step mechanism. A computational mesh of 366x54 is adopted in the simulations.

All computations were performed on an AMD Athlon™ X2 5000. For all cases a relative convergence of 10^{-5} was specified. The grid effects on the solutions were examined by increasing the number of nodes and verifying the solutions until the results no longer changed in a specified tolerance.

4. RESULTS AND DISCUSSION

The parameters for the one-step global mechanism used as a first approximation are the same to all cases. The activation energy, Ea, and the pre-exponential factor, A, were taken from Mohamad et al. (1994) and are $140x10^3$ J/mol and $1x10^{10}$ $m^3kg^{-1}s^{-1}$, respectively. A sensitivity analysis is presented with respect to: Rosseland mean attenuation coefficient, thermal conductivity of the solid and porosity. It was considered the burner developed by Pereira (2002) as the reference and the properties were perturbed ±50% with respect to it in the two porous regions, pre-heating region and combustion region.

4.1. Burner simulated

Figure 2 presents a two-dimensional axisymmetric geometry corresponding to the porous

media burner developed and tested at UFSC-Universidade Federal de Santa Catarina (Pereira, 2002).

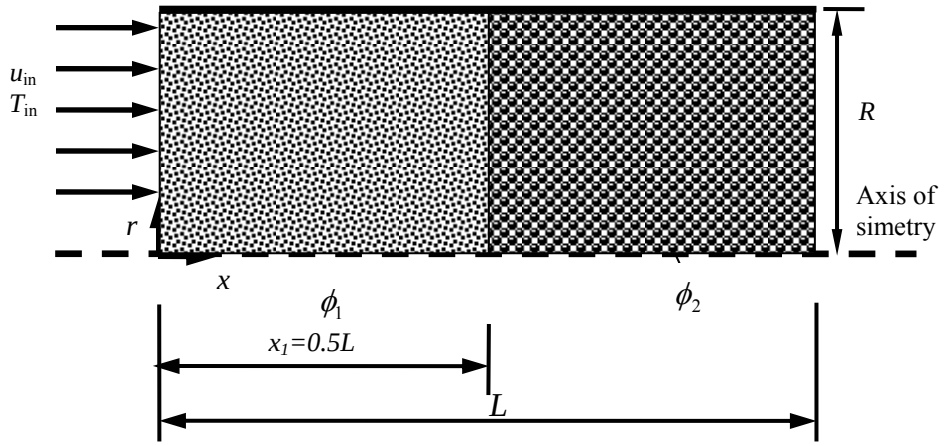

Figure 2. Geometry of a cylindrical porous burner and coordinate system.

The reactor consists of two distinct regions with different porosities and permeabilities, the gas mixture enters at the inflow boundary on the left (preheating region), and the combustion products leave the burner at the outflow boundary on the right (combustion region). In the preheating region a mixture of 65% of zirconium oxide (ZrO_2) and 35% of alumina (Al_2O_3) was utilized, 15.74 pores per centimeter (ppcm), and 86% of porosity. In the combustion region the same material of the preheating region was utilized, with 3.9 ppcm, and 90% of porosity. The walls are impermeable and isolated with a mix of alumina (Al2O3). The numerical parameters are found in table 1.

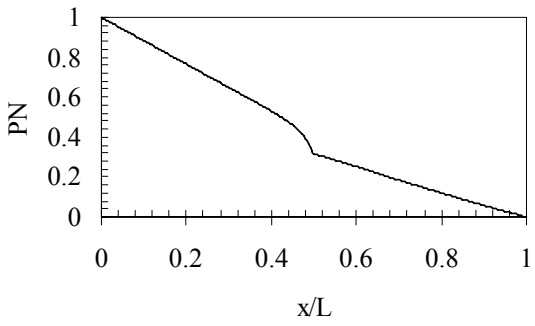

Figure 3. Pressure drop at the center line of the combustor, u_{in}=0.4 m/s

Figure 3 presents the normalized pressure drop at the center line of the combustor, the inflection point represents the interface between the two porous materials. The pressure drop in the first material is larger than in the second due to the lower permeability in the first porous matrix. The 2D temperature field is presented in figure 4. No numerical artifice was used in the stabilization process, the flame stabilized according to the energy balance, rate of reaction and flow velocity.

Figure 5 presents the temperature, mass fraction of fuel, volumetric rate of fuel consumption profiles and a comparison with an experiment obtained by Pereira (2002) for a two-dimensional axisymmetric geometry with an inlet velocity of 0.40 m/s, an excess air ratio

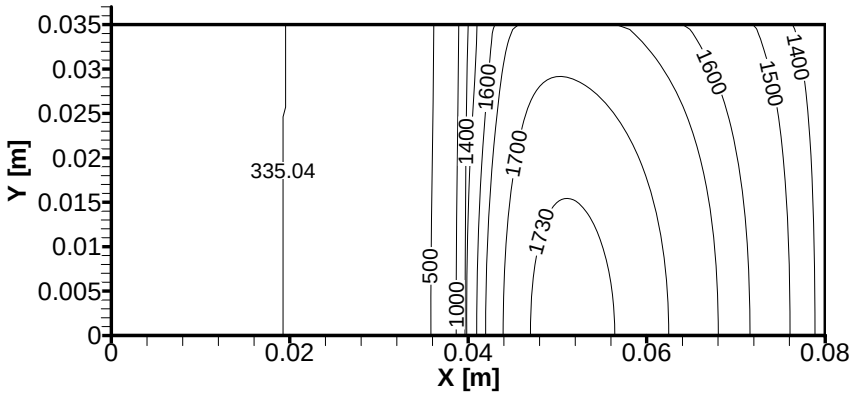

Figure 4. Field of predicted temperature (K), equivalence ratio of 0.60, u_{in}=0.4 m/s.

of 0.67, and an inlet temperature of 335 K. The values for the one dimensional plots were taken at the center line of the combustor. Figure 5 presents two curves, T1 and T2, obtained experimentally (Pereira, 2002) and they are related with two lines of thermocouples in different positions.

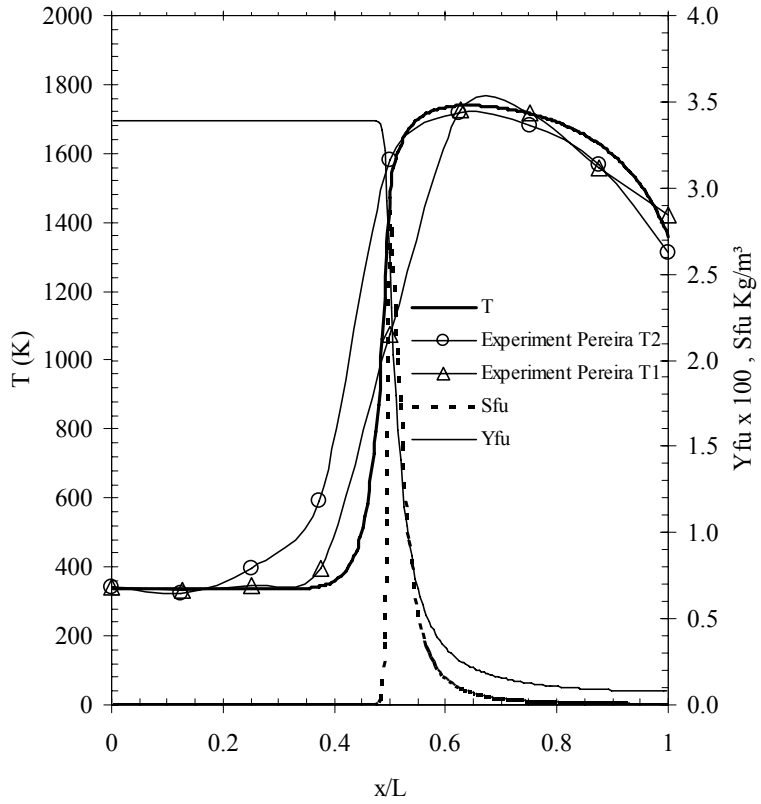

Figure 5. Axial temperature, mass fraction of fuel, volumetric rate of fuel consumption profiles, and a comparison with temperature fields obtained experimentally by Pereira, r/R=0.5, Φ=0.67, u_{in}=0.4 m/s.

The profiles indicate that the effect of the porous matrix on the flame structure is the increase of the flame thickness due to the high conductibility of the solid phase. The experimental results show that the simulation is not considering the right thermal diffusivity,

it is necessary to investigate the thermo-physical properties of the composites utilized in these experiments, there is a high degree of uncertainness about the properties.

4.2. Sensitivity analysis

The sensitivity analysis presented in this section was performed considering the reactor described in the section 4.1 as the reference case. The Rosseland mean attenuation coefficient, K_r, was perturbed ±50 percent in the porous region one and two. The influence of the variations of K_r on the CO emissions at the exit of the reactor, were higher with respect to porous region two (combustion region). Increasing the K_r 50%, in the porous region two, causes an increase on the CO emissions at the exit of the reactor of 34%. Decreasing the K_r 50%, in the porous region two, causes a decrease on the CO emissions at the exit of the reactor of 25%. The influence of the variations of K_r of the matrix one (pre-heating region) is negligible, -0.2% and 1%, increasing K_r and decreasing K_r, respectively. Figure 6 displays the calculated results of CO mass fraction profiles at the centerline of the reactor for the perturbed values of Rosseland mean attenuation coefficient at the preheating region and combustion region, represented by the numbers 1 and 2, respectively.

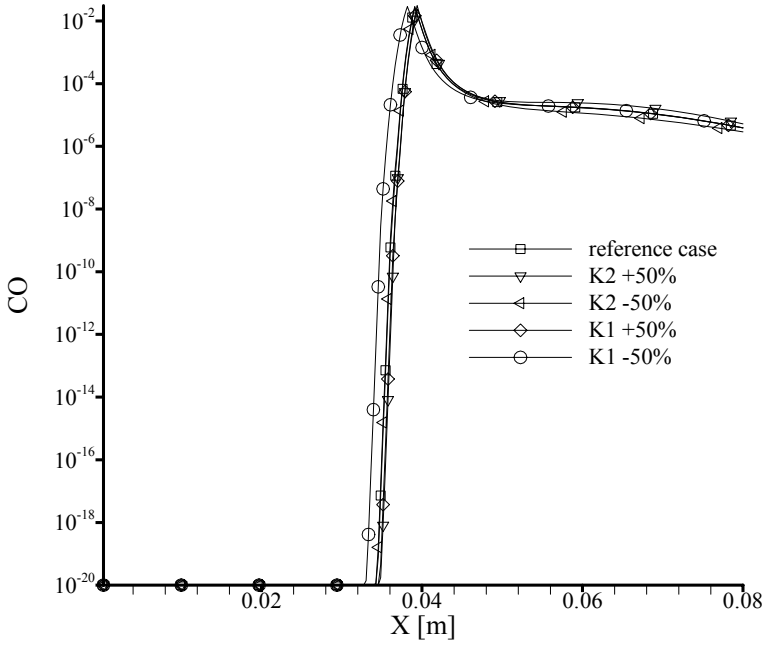

Figure 6. Calculated CO mass fraction profiles at the centerline of the combustor perturbing the Rosseland mean attenuation coefficient ±50% in the porous region one and two.

When the thermal conductivity of the solid, k_s, is increased of 50% in the porous region two, a decrease on the CO emissions at the exit of the reactor of 15.7% is reached. Decreasing the k_s of the porous region two 50% causes an increase on the CO emissions at the exit of the reactor of 20.4%. The influence of the variations of k_s of the matrix one (pre-heating region) is negligible, 0.4% and -0.3%, increasing k_s and decreasing k_s, respectively. Figure 7 presents the calculated results of CO mass fraction profiles at the centerline of the reactor

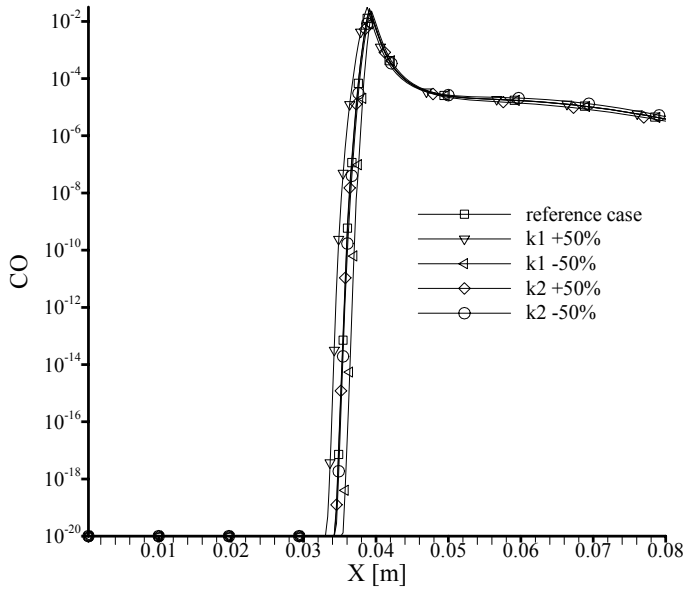

Figure 7. Calculated CO mass fraction profiles at the centerline of the combustor perturbing the thermal conductivity of the solid ±50% in the porous region one and two.

for the perturbed values of thermal conductivity of the solid at the preheating region and combustion region. The peak of CO occurs close to the interface between the two porosity blocks.

The decrease of the porosity has an effect similar to the increase of thermal conductivity as can be seen at the figure 8. A decrease of the porosity of 3.5% on the region two (combustion region), causes a decrease on the CO emissions at the exit of the reactor of 9.3%. An increase of porosity of 3.5% on the region two, causes an increase of 10.3% on the CO emissions at the exit of the reactor. The influence of the variations of the porosity of the matrix one (pre-heating region) is negligible, less than 1%.

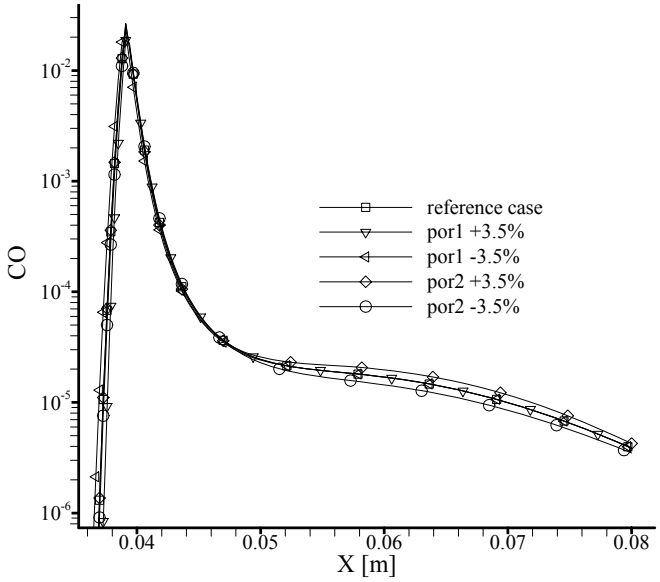

Figure 8. Calculated CO mass fraction profiles at the centerline of the combustor perturbing the porosity ±3.5% in the porous region one and two.

The CO mass fraction variations obtained perturbing the Rosseland mean attenuation coefficient, the thermal conductivity of the solid and the porosity are summarized at the table 2. Additionally, are presented at the figures 9, 10 and 11 the influence of the variations of k_s of the matrix one and two on the mass fraction profiles of the species OH, H_2 and CH_4, respectively.

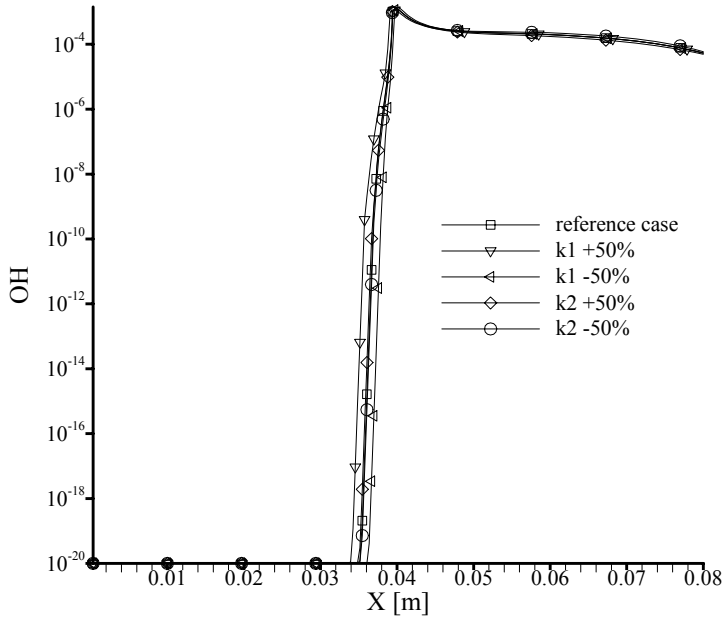

Figure 9. Calculated OH mass fraction profiles at the centerline of the combustor perturbing the thermal conductivity of the solid ±50% in the porous region one and two.

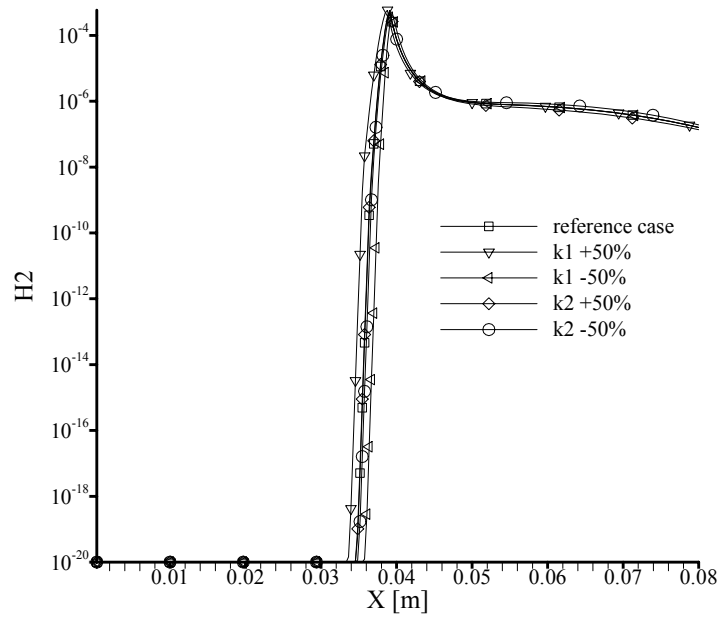

Figure 10. Calculated H2 mass fraction profiles at the centerline of the combustor perturbing the thermal conductivity of the solid ±50% in the porous region one and two.

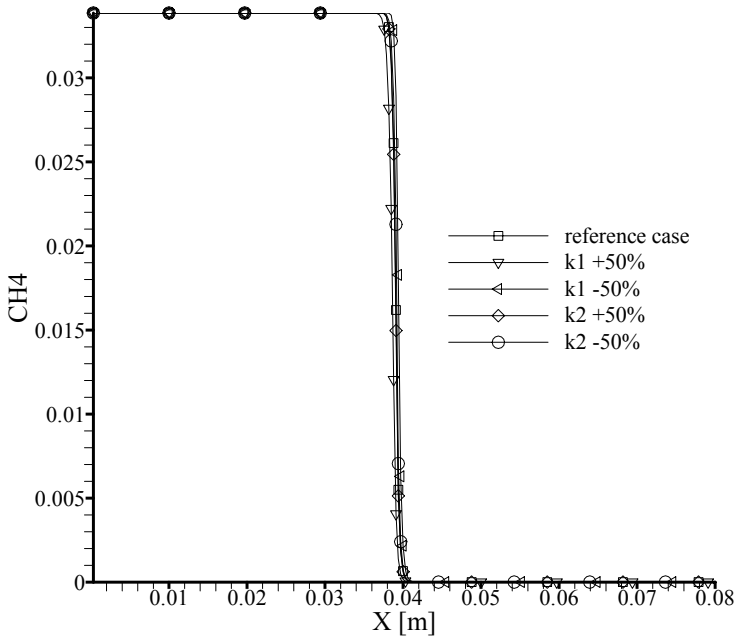

Figure 11. Calculated CH4 mass fraction profiles at the centerline of the combustor perturbing the thermal conductivity of the solid ±50% in the porous region one and two.

5. CONCLUSION

A mathematical model has been developed, and numerically obtained results compared with available experimental data. Temperature, mass fraction of some species, flame location, and pressure drop have been predicted. Numerical results compared reasonably well with the experimental data, in spite of the high uncertainty about the thermal physical parameters.

The model can be used to predict the fields of temperature, mass fraction of the species, pressure drop, and velocity. There are a lot of properties of the composites that need to be more investigated experimentally. There is a high uncertainness about porosities, thermal physical properties, radiative properties, etc. The variations of these properties affect the flame stabilization position and all the variables fields, better is the precision of the values of the physical properties, better results will be obtained.

The sensitivity analysis showed that the material utilized at the combustion region has a stronger influence on the pollutants emission at the exit of the reactor. The properties of the pre-heating region not affect, significantly, the pollutants emission.

6. ACKNOWLEDGEMENTS

The authors are thankful to CNPQ, Brazil, for their financial support during the preparation of this work, and to thank Dr. Carla S. Tafuri Marques and the IEAV - Instituto de Estudos Avançados for the license acquisition of Chemkin 4.1 and the permission to the authors to use it.

Quantity	Value
Length of the combustor chamber – L(cm)	8
D (cm)	7
P_0 (kN/m2)	101.325
Porosity1	0.86
Porosity2	0.90
Inlet gas temperature (K)	335
$k_{s,1}$ (W/mK)	5.0
$k_{s,2}$ (W/mK)	20.0
ε_{eff}	1.0

Table 1. Operating Conditions

	Preheating region		**Combustion Region**	
	+50%	**-50%**	**+50%**	**-50%**
$\mathbf{k_s}$	0.4%	-0.3%	-15.7%	20.4%
$\mathbf{K_r}$	-0.2%	1.0%	34.0%	-25.0%
	+3.5%	**-3.5%**	**+3.5%**	**-3.5%**
$\boldsymbol{\phi}$	-0.1%	0.1%	10.3%	-9.3%

Table 2. Maximum difference in the CO mass fraction at the exit of the reactor obtained with the perturbed properties

7. REFERENCES

Baek, S. W., 1989, "The Premixed Flame in a Radiatively Active Porous Medium," Combust. Sci. Technol., 64, pp. 277–287.

Bear, J., Dynamics of Fluids in Porous Media, New York: Dover, 1972.

Chang, W.C., and Chen, J.Y., Reduced Mechanisms based on GRI-Mech 1.2, http://firebrand.me.berkeley.edu/griredu.html

Howell, J. R., Hall, M. J., and Ellzey, J. L., 1996, "Combustion of Hydrocarbon Fuels Within Porous Inert Media," Prog. Energy Combust. Sci., 22, pp. 121–145.

Hsu, P.-F., Howell, J. R., and Matthews, R. D., 1993, "A Numerical Investigation of Premixed Combustion Within Porous Inert Media," ASME J. of Heat Transfer, 115, pp. 744–750.

Kaviany. M.. 1995. Principles of Heat Transfer in Porous Media. 2nd edn. Springer. New York.

Kee, R. J., Rupley, F. M., Miller, J. A., Coltrin, M. E., Grcar, J. F., Meeks, E., Moffat, H. K., Lutz, A. E., Dixon-Lewis, G., Smooke, M. D., Warnatz, J., Evans, G. H., Larson, R. S., Mitchell, R. E., Petzold, L. R., Reynolds, W. C., Caracotsios, M., Stewart, W. E., Glarborg, P., Wang, C., McLellan, C. L., Adigun, O., Houf, W. G., Chou, C. P., Miller, S. F., Ho, P., Young, P., Young, D. J., CHEMKIN Release 4.0, Reaction Design, San Diego, CA (2004).

Kee, R. J., Rupley, F. M., Miller, J. A., Coltrin, M. E., Grcar, J. F., Meeks, E., Moffat, H. K., Lutz, A. E., Dixon-Lewis, G., Smooke, M. D., Warnatz, J., Evans, G. H., Larson, R. S., Mitchell, R. E., Petzold, L. R., Reynolds, W. C., Caracotsios, M., Stewart, W. E., Glarborg, P., Wang, C., Adigun, O., Houf, W. G., Chou, C. P., and Miller, S. F., Thermodynamic data

is part of the CHEMKIN Collection. Chemkin Collection, Release 3.7, Reaction Design, Inc., San Diego, CA (2002).

Malico, I., Zhou, X.Y., and Pereira, J.C.F., 2000, Two-dimensional Numerical Study of Combustion and Polutants Formation in Porous Burners, Com,bust. Sci. and Tech., 152, pp. 57-79.

Mesquita, M.S., 2003, Análise da dispersão mássica em meios porosos em regimes laminar e turbulento. Tese de doutorado, Instituto Tecnológico de Aeronautica, Brasil.

Mohamad, A.A., Ramadhyani, S., Viskanta, R, 1994.Modeling of Combustion and Heat-Transfer in a Pcked-Bed with Embedded Coolant Tubes, Int. J Heat and Mass Transfer. vol. 37. (8) pp.1181-1191.

Moro Filho, R. C.; Pimenta, Amilcar . A numerical study of combustion in porous burner with a two-energy equation model, Gramado-RS, 20th International Congress of Mechanical Engineering, 2009.

Neef, M., Knaber, P., Summ, G., 1999, Numerical Bifurcation Analysis of Premixed Combustion in Porous Inert Media, unpublished, http://citeseer.csail.mit.edu/197085.html

Pantangi, V. K. and S.C. Mishra, Combustion of gaseous hydrocarbon fuels within porous media – National Conference on Advances in Energy Research, 4-5 December 2006, IIT Bombay.

Patankar. S. V.,1980. Numerical Heat Transfer and Fluid Flow. Hemisphere. New York.

Pedras, M.H.J., 2000, Análise do Escoamento Turbulento em Meio Poroso Descontínuo. Tese de doutorado, Instituto Tecnológico de Aeronautica, Brasil.

Pereira, F.M., 2002, Medição de características térmicas e estudo do mecanismo de estabilização de chama em queimadores porosos radiantes. Tese de Mestrado, Universidade Federal de Santa Catarina, Brasil.

Rocamora, F.D.J., 2001, Análise do transporte de calor em regime laminar e turbulento em meio poroso descontínuo. Tese de doutorado, Instituto Tecnológico de Aeronautica, Brasil.

Sathe, S.B., Peck, R.E., and Tong, T.W., 1990, Flame Stabilization and Multimode Heat Transfer in Inert Porous Media: A Numerical Study, Combust. Sci. and Tech., Vol. 70, pp. 93-109.

Siegel, Robert, and, Howell, John, 2002, Thermal Radiation Heat Transfer, 4th edition.

Stone, H. L., 1968, Iterative Solution of Implicit Approximations of Multidimensional Partial Equations, SIAM J. Numer. Anal. vol 5, pp. 530-558.

Trimis, D., and, Durst, F., 1996, Combustion in a Porous Medium Advances and Applications, Combust. Sci. Technol, Vol. 121, pp. 153-168.

Weinberg, F. J., 1971, Combustion Temperatures: the future?, Nature, 233, 239-241.

Yanenko, N. N. (l97l). The method of fractional time steps: the solution of problems of'mathematical phisics in several variables, M . Holt (Editor), Springer-Verlag, New York.

Yoshizawa, Y., Sasaki, K., and Echigo, R., 1988, "Analytical Study of the Structure of Radiation Controlled Flame," Int. J. Heat Mass Transf., 31, pp. 311–319. [Inspec] [ISI]